MEASUREMENT OF THE ANTIQUARK FLAVOR ASYMMETRY IN THE NUCLEON SEA

by

RUSTY SHANE TOWELL, B.S.

DISSERTATION

Presented to the Faculty of the Graduate School of

The University of Texas at Austin

in Partial Fulfillment

of the Requirements

for the Degree of

DOCTOR OF PHILOSOPHY

THE UNIVERSITY OF TEXAS AT AUSTIN

December 1998

Table of Contents

Chapter 1

Introduction

The history of the study of the building blocks of matter is a series of discoveries of diminishingly smaller pieces which are increasingly more tightly bound and composed of fewer constituents. The starting point could be considered to be the discovery of molecules. All compounds are composed of weakly bound molecules of which there are a plethora of types. Next came the discovery that molecules are composed of atoms. Then as machines were made that could probe matter at higher energies and correspondingly smaller sizes, it was understood that atoms had internal structure and were made of protons, neutrons, and electrons.

The discovery of large numbers of mesons, heavier hadrons, and anti-particles indicated that there was some smaller, more basic building blocks yet to be discovered. These smallest, most tightly bound, and relatively few building blocks are described by the standard model. This model of only 12 different types of quarks and 12 different types of leptons appears to explain the composition of all matter. In fact most of the matter we interact with every day is made of only 2 different types, or flavors, of quarks and a single flavor of leptons.

The bulk of the matter around us is composed of nucleons and electrons.

Electrons are currently believed to be fundamental particles with no discernible internal structure. Nucleons on the other hand, are composed of the two lightest quarks, the up quark and the down quark. Nucleons composed of two up quarks and one down quark are protons. Nucleons composed of one up quark and two down quarks are neutrons.

The parton model describes the nucleon as a bound state of three quarks that give the nucleon its electrical charge and other basic properties. These three quarks, called valence quarks, are held together by the strong force which is mediated, or carried, by gluons. In addition to valence quarks and gluons, there is a background of quark-antiquark pairs which come and go without affecting the basic characteristics of the nucleon since any effect of the quark is canceled out by the opposite effect of the antiquark. These components of the nucleon, shown in figure 1.1, are collectively referred to as partons.

According to the theoretical description of the strong force, quantum chromodynamics (QCD), a source of these quark-antiquark pairs, commonly called the sea quarks, is gluon splitting. A gluon can split into a quark-antiquark pair which exists for a while before they recombine back into a gluon. This simple production mechanism implies that the sea of antiquarks in a nucleon would be flavor symmetric with respect to the up and down anti-quarks. Therefore it was long assumed that there were as many anti-up quarks in a nucleon as there were anti-down quarks.

Over the past decade evidence has built to the point were, even though it wasn't understood, it was generally believed that there were more anti-down quarks in a proton than anti-up quarks. This was the primary motivation for Experiment 866 at Fermi National Accelerator Laboratory (FNAL

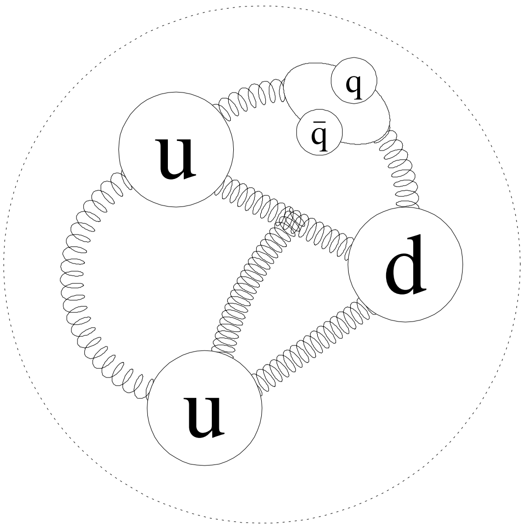

Figure 1.1: A simple picture of the proton according to the parton model. The proton contains 2 valence up quarks (u), one valence down quark (d), gluons (helix), and the sea of quark anti-quark pairs (q and $\bar{q}$).

E866/NuSea). This experiment, also known as NuSea, has extensively measured for the first time the antiquark content of the nucleon sea.

Chapter 2

Theory and Motivation

The structure of the nucleon is difficult to study because of the small size and large binding energy. However, much has been learned about the structure of the nucleon in recent years with the aid of particle accelerators. Two electromagnetic interactions which can be studied at the high energies produced by modern accelerators, are deep inelastic scattering and the Drell-Yan process. These two methods of probing the nucleon have revealed much about the nucleon sea.

2.1 Deep Inelastic Scattering

Deep inelastic scattering (DIS) is the process, shown in figure 2.1, where a high energy charged lepton is inelastically scattered off of a target nucleon. In this process the lepton scatters off a single quark in the nucleon by exchanging a high energy virtual photon. The differential cross section for this interaction can be measured experimentally and expressed in terms of the two structure functions $F_1(x, Q^2)$ and $F_2(x, Q^2)$. These structure functions are functions of Bjorken-x (x) which is a dimensionless scaling variable that at high energies represents the fraction of the nucleon's longitudinal momentum carried by a parton and Q^2 which is the four momentum squared of the virtual photon

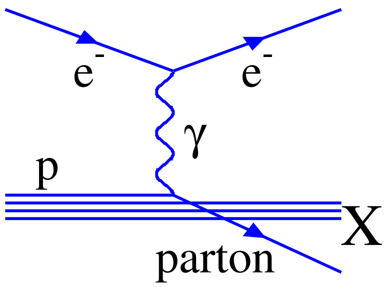

Figure 2.1: Deep inelastic scattering.

exchanged in the process.

These two structure functions can be expressed as linear combinations of parton functions. These parton functions, $f_i(x, Q^2)$, which are commonly called parton distribution functions (PDF), are also functions of x and Q^2. These PDF's are the probability of finding a parton in the nucleon which carries some fraction (x) of the nucleons total longitudinal momentum. The relationship between the structure functions and the PDF's is:[1]

$$F_1(x) = \frac{1}{2}\sum_i e_i^2 f_i(x) \tag{2.1}$$

$$F_2(x) = \sum_i e_i^2 x f_i(x). \tag{2.2}$$

Where the sum is over all of the partons ($i = u, d, s, ..., \bar{u}, \bar{d}, \bar{s}, ..., g$) and e_i is the electrical charge of the i-th parton. So from measuring the cross section for DIS, one can get information about the internal structure of the nucleon.

An experiment performed by the New Muon Collaboration (NMC) measured the cross section ratio for deep inelastic scattering of muons off of hydrogen and deuterium. Their measurement [2] of $F_2^{\mu n}/F_2^{\mu p}$ over the kinematic range

[1]Since the Q^2 dependence is small, it will be ignored through most of this thesis.
[2]NMC actually measured $F_2^d/F_2^p \equiv 1/2(1 + F_2^n/F_2^p)$.

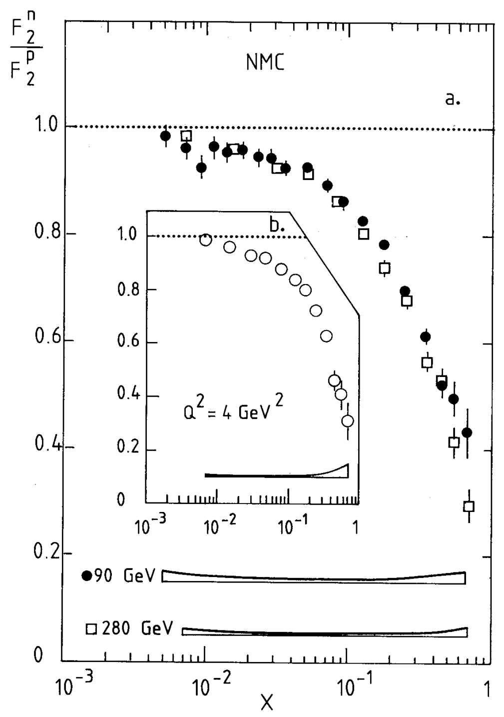

Figure 2.2: (a) The ratio F_2^n/F_2^p as a function of x averaged over Q^2 as measured at 90 GeV and 280 GeV incident muon energy. (b) The ratio F_2^n/F_2^p at $Q^2 = 4\ \mathrm{GeV}^2$. The bands show the systematic uncertainties.

of $0.004 < x < 0.8$ is shown in figure 2.2a as measured at 90 GeV and 280 GeV incident muon energy. These data points are averaged over Q^2 which changes from point to point. Figure 2.2b is the result of combining both measurements and evolving the data to a fixed Q^2 of 4 GeV.

This measurement by NMC was used with a parameterization of the absolute deuteron structure function, F_2^d to obtain

$$F_2^p - F_2^n = 2F_2^d \frac{1 - F_2^n/F_2^p}{1 + F_2^n/F_2^p}. \tag{2.3}$$

Figure 2.3 show the derived value of $F_2^{\mu p} - F_2^{\mu n}$ as a function of x in the solid

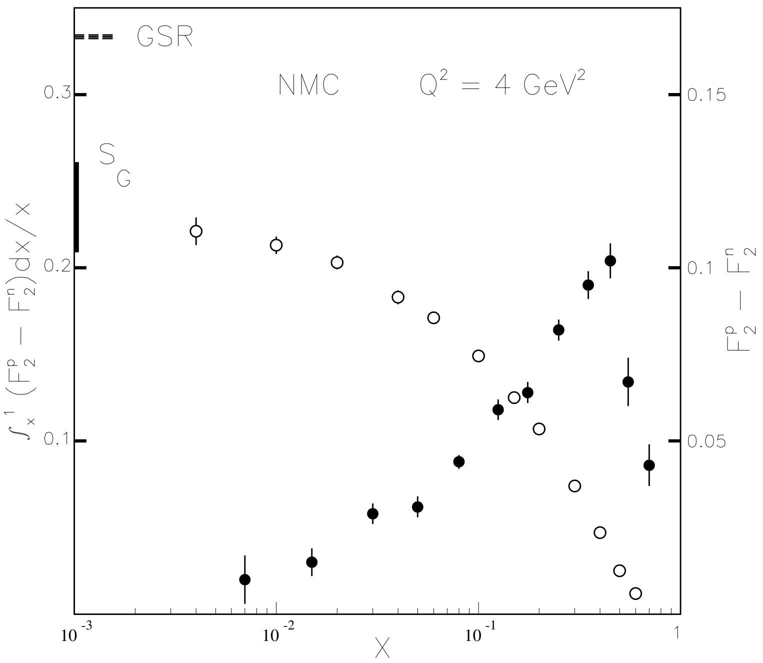

Figure 2.3: The difference $F_2^p - F_2^n$ (solid symbols and the scale to the right) and $\int_x^1 (F_2^p - F_2^n)dx/x$ (open symbols and the scale to the left) at $Q^2 = 4$ GeV^2 as a function of x. The extrapolated integral result, S_G is indicated by the bar. The traditional Gottfried Sum Rule result, GSR is also shown.

points. Also shown in this figure is the integral of $(F_2^{\mu p} - F_2^{\mu n})/x$ for the same x range. To compare this measurement with the Gottfried Sum Rule they extrapolated this result to cover all values of x $(0 \leq x \leq 1)$. This resulted in a measured value for the Gottfried Sum (S_G) of

$$S_G \equiv \int_0^1 [F_2^{\mu p} - F_2^{\mu n}] \frac{dx}{x} = 0.235 \pm 0.026. \tag{2.4}$$

This result is much less than the traditional Gottfried Sum Rule (GSR) result of 1/3. To understand this discrepancy between the NMC measurement and the traditional result of the Gottfried Sum Rule, it is important to look at the assumptions that lead to the traditional result. Start with the Gottfried sum as written in equation 2.4 and then use equation 2.2 to get

$$S_G = \int_0^1 \sum_i e_i^2 \left[q_i^p(x) + \bar{q}_i^p(x) - q_i^n(x) - \bar{q}_i^n(x)\right] dx. \tag{2.5}$$

Next assume charge symmetry to express the neutron PDF's as proton PDF's and ignore the heavier quark terms to get

$$S_G = \int_0^1 \frac{1}{3}\left[u + \bar{u} - d - \bar{d}\right] dx \tag{2.6}$$

which can be rewritten as

$$S_G = \int_0^1 \frac{1}{3}\left[u - \bar{u}\right] dx - \int_0^1 \frac{1}{3}\left[d - \bar{d}\right] dx + \int_0^1 \frac{2}{3}\left[\bar{u} - \bar{d}\right] dx. \tag{2.7}$$

The first two integrals are just the definition of valence quarks, which for a proton is 2 up valence quarks and one down valence quark. So equation 2.7 can be reduced to

$$S_G = \frac{1}{3} + \int_0^1 \frac{2}{3}\left[\bar{u} - \bar{d}\right] dx. \tag{2.8}$$

Now if it is assumed that $\bar{d}(x) = \bar{u}(x)$ then one arrives at the traditional result of 1/3.

To reconcile the NMC measurement and the traditional Gottfried Sum result, one of three assumptions made above must be wrong. First is the assumption that the NMC measurement can be extrapolated to zero. Second is the assumption that charge symmetry is valid and the third assumption is that $\bar{d}(x) = \bar{u}(x)$. The small x extrapolation was checked by Fermilab E665 which made the same measurement as NMC except they measured the ratio for $10^{-6} \le x \le 0.3$. Nothing was seen which indicated the extrapolation made by NMC was invalid. Charge symmetry is know not to be a perfect symmetry, but it is in general good to the proton neutron mass difference which is much smaller than the discrepancy here.

So that leaves the assumption that $\bar{d}(x) = \bar{u}(x)$. If this assumption is solely responsible for the discrepancy between the NMC measurement and the traditional Gottfried Sum Result then it would imply that

$$\int_0^1 [\bar{d}(x) - \bar{u}(x)]dx = 0.148 \pm 0.039. \tag{2.9}$$

It was this measurement that first indicated that there were more anti-down quarks in the proton than anti-up quarks.

2.2 Drell-Yan

Following the publication of the NMC result, it was suggested that the Drell-Yan process could be used as a more direct probe of the light antiquark asymmetry of the nucleon. In its simplest form, shown in figure 2.4, the Drell-Yan process is the production of a lepton-antilepton pair from a virtual photon produced in quark-antiquark annihilation. Since there are no valence antiquarks in a nucleon-nucleon interaction, the Drell-Yan process is a direct probe of the sea quarks.

The proton-nucleon cross section for the Drell-Yan process, to lowest order in the electromagnetic fine structure constant (α), as a function of x of the initial quark and anti-quark is

$$\frac{d^2\sigma}{dx_1 dx_2} = \frac{4\pi\alpha^2}{9M^2} \sum_i e_i^2 \left[f_i(x_1)\bar{f}_i(x_2) + \bar{f}_i(x_1) f_i(x_2) \right], \tag{2.10}$$

where the sum is over all quark flavors and M is the dilepton mass. Here the subscript 1 denotes a parton from the beam and 2 denotes a parton from the

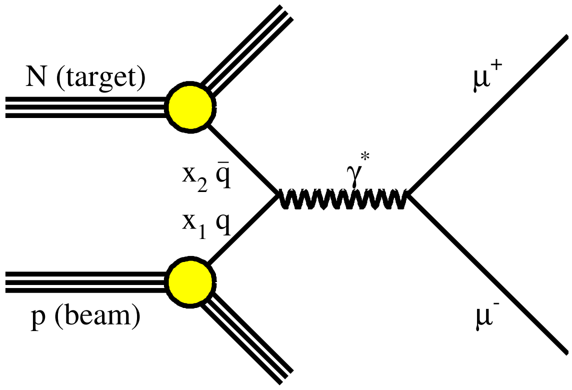

Figure 2.4: The leading order Drell-Yan process.

target. It is important to note that the PDF's in equation 2.10 are the same functions used in equation 2.2 which means that DIS and the Drell-Yan process are sensitive to the same anti-quark structure of the nucleon.

Some kinematic quantities commonly used in describing a Drell-Yan event are the x Feynman (x_F) and the dilepton mass (M) which are defined [3] as

$$x_F = p_{||}^{\gamma}/p^{\gamma,max} \approx x_1 - x_2 \tag{2.11}$$

$$M^2 = Q^2 \approx x_1 x_2 s \tag{2.12}$$

where $p_{||}^{\gamma}$ is the center of mass longitudinal momentum of the virtual photon, $p^{\gamma,max}$ is its maximum possible value, and s is the total four momentum squared of the initial nucleons. Additionally the transverse momentum (p_T) of the dileptons is also used to complete [4] the description of the event.

[3]The approximations in these equations become exact in the infinite momentum frame.
[4]The complete event description includes production and decay angles but that will not be included here.

The cross section for producing a Drell-Yan event in a proton-proton interaction, σ^{pp}, or proton-neutron interaction, σ^{pn} is,

$$\sigma^{pp} \propto \frac{8}{9}u(x)\bar{u}(x) + \frac{2}{9}d(x)\bar{d}(x) \tag{2.13}$$

$$\sigma^{pn} \propto \frac{5}{9}u(x)\bar{u}(x) + \frac{5}{9}d(x)\bar{d}(x) \tag{2.14}$$

where the heavier quark terms have been ignored, charge symmetry has been invoked[5] so that all the PDF's are proton PDF's and x_F is zero[6]. Since there are no free neutron targets, deuterium is commonly used as the best approximation to a free neutron target. Making the approximation that the proton deuterium cross section (σ^{pd}) can be written as,

$$\sigma^{pd} \approx \sigma^{pp} + \sigma^{pn} \tag{2.15}$$

obviously ignores the small [7] nuclear affects inside the deuterium nucleus. Using this good approximation the measured cross section ratio can be written as,

$$\left.\frac{\sigma^{pd}}{\sigma^{pp}}\right|_{x_1=x_2} = \frac{8 + 5\frac{\bar{d}}{\bar{u}} + 5\frac{d}{u} + 2\frac{\bar{d}}{\bar{u}}\frac{d}{u}}{8 + 2\frac{\bar{d}}{\bar{u}}\frac{d}{u}} \tag{2.16}$$

where the notation showing the x dependence has been dropped. From this quantity that can be measured, one can solve for $\bar{d}/\bar{u}$,

$$\frac{\bar{d}}{\bar{u}} = \frac{8\left(1 - \frac{\sigma^{pd}}{\sigma^{pp}}\right) + 5\frac{d}{u}}{2\frac{d}{u}\left(\frac{\sigma^{pd}}{\sigma^{pp}} - 1\right) - 5}. \tag{2.17}$$

So by measuring the Drell-Yan cross sections, the nucleon sea can be measured.

The NA51 collaboration at CERN used this idea. They used the primary proton beam from the CERN-SPS to produce 450 GeV/c protons which

[5] Charge symmetry implies that $u_p(x) = d_n(x)$, $\bar{d}_p(x) = \bar{u}_n(x)$, etc.

[6] The reason for this simplification is so that this discussion can be compared to the NA51 measurement.

[7] E772 searched for nuclear effects in Drell-Yan production and found none.

interacted in one of three identical vessels which contained liquid hydrogen, liquid deuterium or a vacuum. From the almost six thousand reconstructed Drell-Yan events with a mass above 4.3 GeV/c^2 they determined,

$$\left.\frac{\bar{u}_p}{\bar{d}_p}\right|_{\langle x\rangle=0.18} = 0.51 \pm 0.04 \pm 0.05. \tag{2.18}$$

This was the first direct determination of $\bar{d}/\bar{u}$, but this measurement was made at only a single x value.

2.3 Global Fits

Various groups of scientist use the results from DIS, Drell-Yan, and other methods of probing the nucleon to generate a set of PDF's. This method of fitting all the relevant data is called a global fit. Two groups that generated global fits parameterizing the nucleon sea were CTEQ and MRS. Prior to the measurements by NMC and NA51, the usual assumption was that $\bar{d}(x) = \bar{u}(x)$. A typical parameterization of the proton with this assumption is shown in figure 2.5.

Prior to FNAL E866/NuSea the main constraints on the global fits of $\bar{d}(x)$ and $\bar{u}(x)$ were the NMC and NA51 results. This parameterizations, shown in figure 2.6, constituted the worlds best guess at the structure of the nucleon sea prior to the measurement reported here.

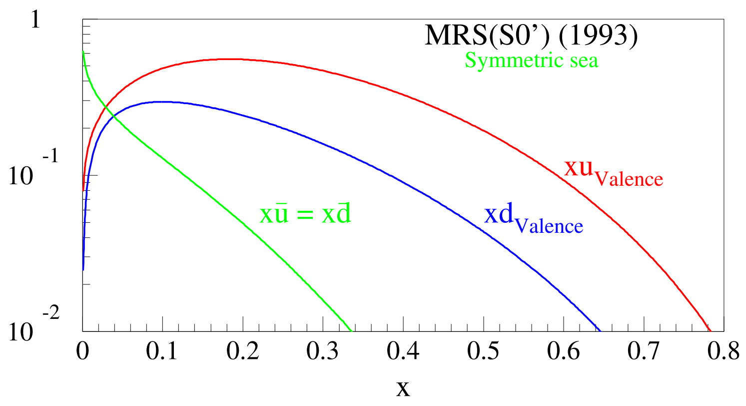

Figure 2.5: Old Parameterization of the proton by MRS assuming a symmetric sea.

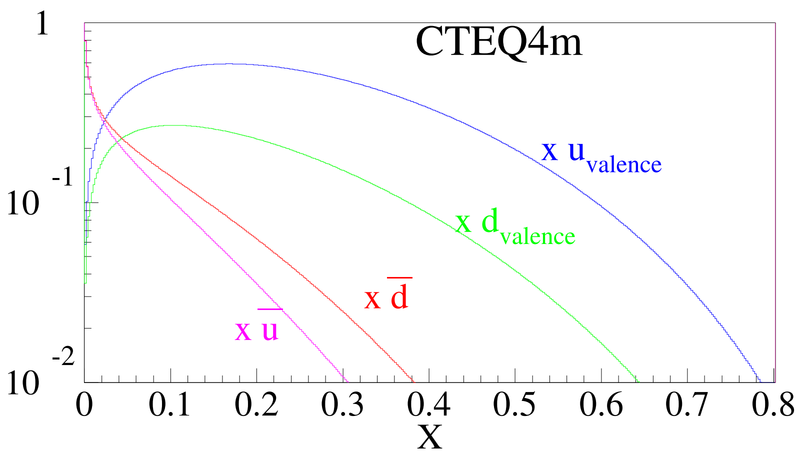

Figure 2.6: Old parameterization of the proton published by CTEQ prior to FNAL E866/NuSea.

Chapter 3

Experimental Setup

The goal of this experiment was to measure the ratio of Drell-Yan events from a proton-proton interaction to a proton-neutron interaction. To count the number of Drell-Yan events it was necessary to detect a pair of high energy oppositely charged muons. To measure this ratio as a function of the kinematics of the interaction, it is necessary to measure the four momentum of each muon produced in the Drell-Yan process. This was accomplished by reconstructing the path of a pair of oppositely charged muons (call a dimuon event) through a series of tracking stations and dipole magnets.

This chapter will describe the experimental apparatus used to make this measurement. The equipment will be described in the order in which a particle would traverse the setup. Starting with a description of the beam, then the targets, and finally the spectrometer. The coordinate system used through out this experiment aligns the positive z-axis with the direction the incoming beam is traveling. The y-axis is oriented with the positive direction pointing up and the x-axis is chosen to complete the right-handed coordinate system.

3.1 Beamline and Beam Monitors

The beam used in this experiment was an 800 GeV/c proton beam extracted from the Fermilab Tevatron accelerator. The beam was extracted slowly over a twenty second time period once a minute. This slow extraction is referred to as a spill. Within each spill the beam arrived in small bunches, called a "bucket", every 19ns. The frequency of the buckets was determined by the radio frequency of the accelerator which was 53 MHz.

As the beam was transported down the East beamline in the meason experimental hall it's size, position, and intensity was monitored with several different detectors. The beam position and size were measured using RF cavities and segmented wire ion chambers (SWIC). The last check of the beam, before it reached the target was performed by a movable SWIC located upstream of the targets about 70 inches. This SWIC had wire spacing of 2mm in the horizontal direction and 0.5mm in the vertical direction. The full width at half maximum size of the beam was typically about 6mm wide and 1mm high.

The beam intensity was monitored by several different detectors. The primary monitor was a secondary emission monitor (SEM) located about 100m upstream of the targets. In addition to the SEM, the beam intensity was also monitored with quarter-wave RF cavities and an ion chamber.

At about 85° from the beam direction in the x-z plane were a pair of four-element scintillator telescopes called AMON and WMON. These scintillator telescopes viewed the target through a hole in the heavy shielding enclosing the targets. The purpose of these detectors was to monitored the luminosity on the target and to determine the beam duty factor, data acquisition livetime and in conjunction with SEM the target position.

3.2 Targets

The 800 GeV/c extracted proton beam struck one of three target flasks. The three identical flasks were cylindrical in shape and 20 inches long by 2.5 inches in diameter. The flasks were constructed of thin stainless steel with an insulated vacuum jacket around each flask. One flask was filled with liquid deuterium, the second was filled with liquid hydrogen, and the third flask was an evacuated flask. The hydrogen target was 7% of and interaction length and 6% of a radiation length long while the deuterium target was 15% of an interaction length and 7% of a radiation length long.

All three flasks were mounted on a movable table so that the target could be changed between spills. The normal target cycle was 12 spills long with 5 spills on the deuterium target, one spill on the empty flask, 5 spills on the hydrogen target and another spill on the empty flask. The electronics that automatically cycled the targets checked that the spill had a SEM count of at least 500 before it counted the spill. This prevented the target from cycling while the accelerator was off. The targets were cycled this frequently so that most of the systematic uncertainties canceled out when the cross section ratio was determined.

3.3 E866 Spectrometer

The primary apparatus used in this experiment was the dimuon spectrometer shown in figure 3.1. This was the fourth experiment to use this spectrometer

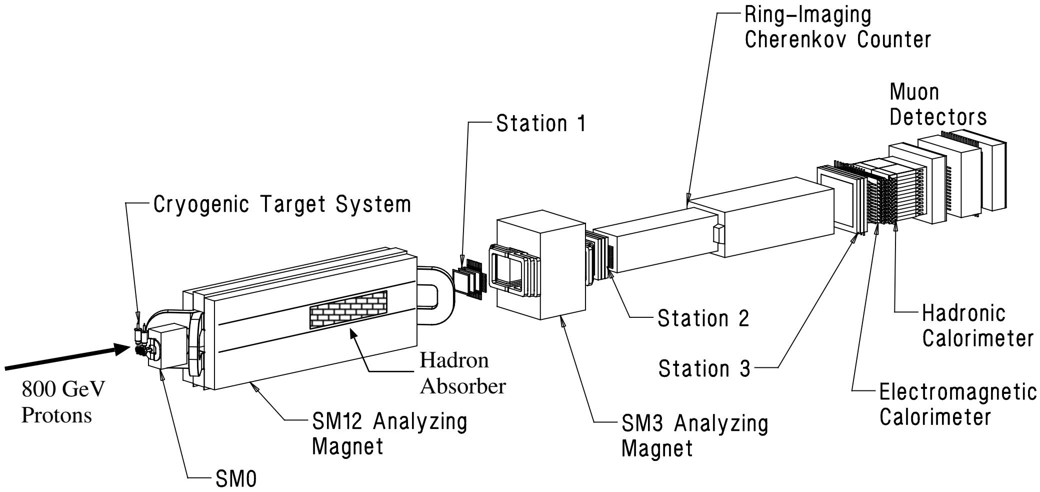

Figure 3.1: The E866 Spectrometer

which is located on the east side of the Meson experimental building at Fermilab. While changes have been made to the spectrometer for each experiment, the basic design has remained the same since the spectrometer was first used for E605 in the early 80's.

Downstream of the targets the particles encountered the first of three dipole magnets. All three magnets used in this spectrometer were dipole magnets with the magnetic field aligned in the x-direction so that they caused charged particles moving in the z direction to bend in the plus or minus y direction.

The first dipole magnet (called SM0) was the smallest magnet measuring 72 inches long and providing a transverse momentum deflection of 0.94 GeV/c when operated at a maximum current of 2100 amps. This magnet was used to increase the opening angle of low mass dimuon pairs when taking data with the magnets configured to have the lowest mass acceptance. The aperture of this magnet was filled with a helium bag. The purpose of this and all other helium bags was to minimize the material that the muons traversed in order to minimize the multiple scattering of the muons and thereby improve track reconstruction.

Immediately following the first dipole magnet was the largest dipole magnet (SM12) which was over 47 feet long. When operated at a maximum current of 4000 amps it provided a transverse momentum deflection of 7 GeV/c. This magnet focused the dimuons through the remainder of the spectrometer. Inside of the aperture of this magnet was a beam dump. The protons which did not interact in the targets, interacted in the 129 inch long copper beam dump which corresponds to about 22 interaction lengths and 230 radiation lengths long. This prevented the beam from passing through the active elements of the spectrometer. The beam dump generally filled the aperture in the x-direction, but was only a maximum of 10 inches thick in the y-direction. This allowed the dimuons of interest to travel above and below the beam dump.

(Add figure of the one event display????????)

At the downstream end of the beam dump was an absorber wall which completely filled the aperture of the magnet in both the x and y directions. This wall, shown in figure 3.2 was built in seven layers. The first layer was 24 inches of copper. This was followed by 4 layers of 27 inch thick carbon. The last 2 layers were composed of 36 inch thick borated polyethylene. The effect of this wall was to absorb most of the hadrons and electrons produced in the target or the beam dump since it was over 13 interaction lengths long. This meant that essentially only muons were allowed to traverse the active elements of the spectrometer allowing a higher beam intensity to be used while still keeping the

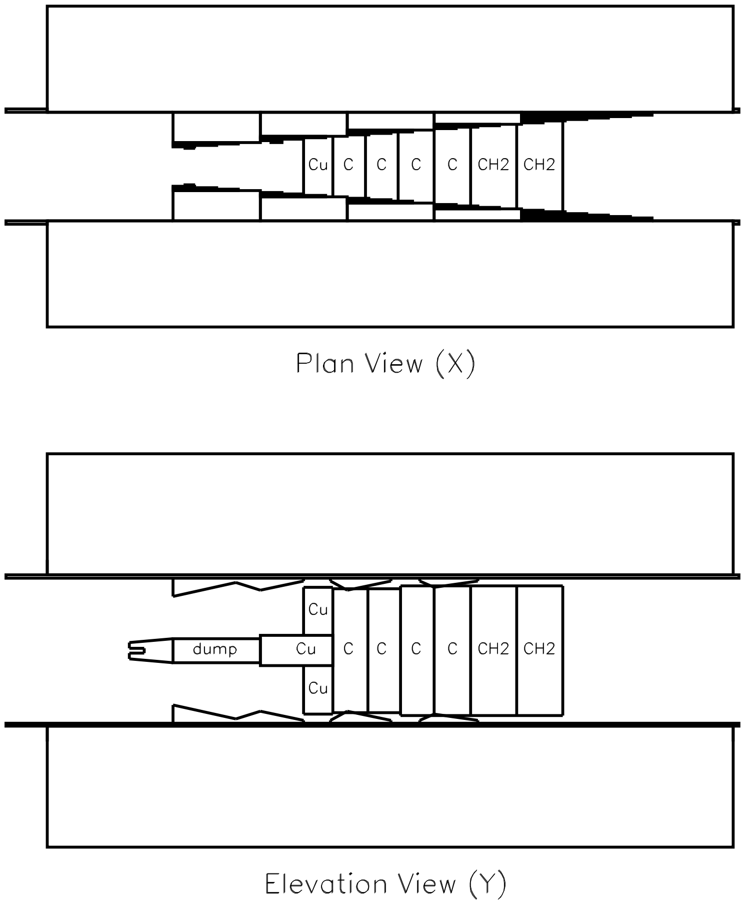

Figure 3.2: The beam dump and absorber wall inside the aperture of SM12

occupancy of the drift chambers at acceptable levels. Following the absorber wall and still inside the aperture of SM12 was another helium bag.

Just downstream of SM12 was the first tracking station. The first three tracking stations were all very similar. Station one consisted of three pairs of drift chambers. The first pair of planes, called u1 and u1$'$ were oriented at approximately $+14^\circ$ ($\arctan\theta = 0.25$) in the x-y plane. The second pair of planes, called y1 and y1$'$, were horizontal so that they measured particle position in the y direction. The third pair of planes, called v and v$'$, were oriented at approximately -14° in the x-y plane. Each pair of planes were offset by half of a drift cell to resolve the ambiguity of the drift direction. These six position measurements were used to track particle very accurately and had enough redundancy built-in to continue to perform well even if some of the channels were inoperative.

While the drift chambers had excellent position resolution, they could not distinguish between beam buckets within a spill and were too slow to use as input to a trigger. Therefore, in addition to the drift chambers, planes of scintillators called hodoscopes were used. The two hodoscope planes at station one, were oriented perpendicular to one another. The plane with horizontal paddles measured the y position and therefore was called the y1 hodoscope. The other plane measured position in the x direction and was called the x1 hodoscope.

After station one was the final dipole magnet called SM3. This magnet had a large aperture measuring about six feet high and five feet wide which was filled with another helium bag. This magnet was always operated at a current of 4230 Amps which provided a transverse momentum deflection of

0.91 GeV/c. Unlike the first two magnets which focused the dimuons into the active elements of the spectrometer, this magnet was a momentum analyzing magnet. The bend in the muon tracks as they passed through this magnet was used to determine the muon momentum.

The second tracking station followed SM3. The second station was a slightly larger version of the first tracking station. Like the first station it also had three pairs of drift chambers (called u2, u2′, y2 ,y2′, v2, and v2′) but unlike the first station, the second station had only one hodoscope (y2) which measured the y position.

As shown in figure 3.1, the second tracking station was followed by a ring imaging cherenkov counter (RICH). This detector was used for particle identification in previous experiments using this spectrometer but was not needed for this experiment. Since the main concern for this experiment was tracking muon pairs, the absorber wall was added to the aperture of SM12 and the RICH was filled with helium to function as a large helium bag.

Downstream of the RICH was the third tracking station. Except for being larger in size, station 3 is identical to station one. It contains three pairs of drift chamber planes and 2 planes of hodoscopes called u3, u3′, y3, y3′, v3, v3′, y3, and x3 respectively.

Like the RICH, the calorimeters that followed station 3 were detectors that were not instrumented for this experiment. These calorimeters served in this experiment only as additional shielding before the station four detectors. Upstream of and between some of the planes in four are large amounts of concrete and zinc shielding. This served as a final barrier to all particles except muons (and of course neutrinos) so station four was also known as the muon detectors.

Since Station 4 was so large and since the additional shielding upstream of station four caused multiple scattering of the muons, the excellent position resolution of drift chambers was not practical or necessary. Therefore proportional tubes were used in place of drift chambers in station four. There were 3 planes of proportional tubes. Two planes measured the y position (pty1 and pty2) and one plane measured the x position (ptx). Station four also had two hodoscope planes (y4 and x4).

3.4 Data Acquisition System

Although much of the data acquisition system (DAQ) was several years old, it was a very fast system. When the trigger fired, the DAQ would write to tape information from the spectrometer and beamline monitors. Additionally, the DAQ would also record to tape information about each beam spill. This section will describe when, how, and what information ended up on tape.

3.4.1 The Trigger

Events were only written to tape when the trigger was satisfied and only if the DAQ was not already busy writing out a previous event that satisfied the trigger. Since the events that were of interest consisted of two muons originating from the target, that was what the trigger looked for.

3.4.2 Readout System

3.4.3 Information Written to Tape

Chapter 4

Experimental Procedures

To complete this experiment required lots of work. This work started years before the first data was taken and continued throughout the year of data taking. This chapter will describe this work. The first section will describe the work that was done to recommission the spectrometer, before the accelerator was turned on. The second section will describe the work that was done to tune up the spectrometer after we started receiving beam, but before data could be taken. The third section will explain the standard data taking procedures while the last section will describe some of the special procedures that were required to be performed periodically.

4.1 Preparing For Beam

The tasks required to prepare the spectrometer to take data fall into one of two categories: recommisioning the existing spectrometer, commissioning the new parts.

4.1.1 Recommisioning The Spectrometer

Many of the detectors, cables, and readout electronics were unchanged from previous experiments that used this spectrometer. However it had laid idol for about 5 years in a rather dirty environment that was subject to very large temperature fluctuations. This fact coupled with the piling of cables off of the counting house roof meant there was lots of work to get the old spectrometer running again.

The cables that carry the signals from the drift chambers to the counting house were 100 wire ribbon cables that were several hundred feet long called Ansley cables. These cables were extra long so that they would act as delays which would give the trigger system longer to make a decision. Since the last experiment to use this spectrometer, these cables were all thrown off of the roof of the counting house and into a pile on the floor of the experimental hall. This was done to satisfy the false fears of safety administrators that the cables were too heavy for the roof.

The connectors at the ends of these cables are large paddles with the wires exposed. The rough treatment of these cables damaged many of them. Therefore after the cables were untangled each wire in each cable was tested and many repairs were necessary. Then the cables were reattached to the detectors, laid back on the roof, and reattached to the read out electronics.

The hodoscopes which were not being replaced were all checked for light leaks. The station 2 hodoscope paddles had become severely misaligned during the past five years and had to be remounted. The signal and high voltage cables were checked, repaired if necessary, and reattached.

All of the electronics from the preamps to the tape drives were tested and repaired if necessary.

4.1.2 Commissioning the new parts of the spectrometer

The spectrometer was upgraded in many areas for this experiment. The station one hodoscopes and drift chambers were replaced with larger detectors to almost double the acceptance of the spectrometer. These detectors had to be designed, built, mounted, aligned, and tested.

The trigger was also completely replaced. The old trigger processor was removed and several new trigger modules were designed, built, installed and tested.

The data acquisition system (DAQ) under went a serious overhaul from its previous configuration. The previous experiment used a PDP-11 to control the DAQ. This was replaced with a VME based system that could handle much higher data rates.

Another dipole magnet (SM0) was added to the front of the spectrometer. Therefore the magnetic fields in both SM0 and SM12 had to be measured. This was done by measuring the magnetic fields on a three dimensional grid throughout the aperture of the magnets.

4.2 Spectrometer tune up with beam

Once the accelerator was turned on and beam was delivered to the meson beam dump we were able to began tuning the spectrometer. The proton beam hitting the beam dump produced enough muons that even though it was about 1400 ft up stream of our spectrometer we could still detect muons. This low flux of muons coming through our spectrometer allowed us to align the hodoscopes and drift chambers as well as test our new trigger and DAQ system.

When beam finally arrived in our area we rechecked the high voltage settings to the hodoscopes and drift chambers. These voltages were optimized to perform at the maximum efficiency without causing too much noise or damaging the detectors. The timing of each hodoscope channel was also checked and adjusted to ensure that all of the hodoscope signals were in coincident with each other. This was critical to ensure that the trigger worked properly.

4.3 Standard Data taking procedures

Though out the year of data taking we constantly monitored the spectrometer, DAQ, beam, targets, magnets, and the gas systems. If any of these systems were performing in an abnormal way, data taking was suspended and the problem was corrected.

Twice a day a shift check was performed. This checked the target pressure and temperature, the drift chamber and proportional tubes gas flow, gas pressure, and high voltages, beam duty factor, and magnet settings.

4.4 special data taking procedures

In addition to the normal daily activities required to take data, additional special measurements where taken periodically. The SEM counter calibration was check using a single beam measurement. Instead of splitting the beam into several separate channels and sending it to different experimental areas at the same time as was usually the practice, the beam was delivered only to our beam line. This allowed the SEM counter in our beamline to be calibrated against the beam intensity monitors in the Tevatron.

Another type of special measurement was a hodoscope efficiency study. Since the normal trigger was not very effective at monitoring the hodoscope efficiency, dedicated runs with a different trigger were necessary. These runs were performed for each data set.

Chapter 5

Analysis

5.1 Data Sets

5.2 First Pass

5.3 Second Pass

5.4 Ntuple Cuts

5.5 Randoms Corrections

5.6 Rate Dependence Correction

Chapter 6

Results and Conclusion

6.1 E866 Results

6.2 Comparison to Theoretical Models

6.3 Future Experiment